Jurnal Teknik Mesin Mechanical Xplore (JTMMX)
Journal homepage: https://journal.ubpkarawang.ac.id/index.php/JTMMX

Original Article

Effect of Post-Weld Heat Treatment Temperature on Microstructure and Mechanical Properties of FCAW-Welded SS400 Steel

Edo Aprianto[1], Haftirman[1]

[1]Department Master of Mechanical Engineering, Faculty of Engineering, Mercubuana University, Jakarta, 11650, Indonesia

ARTICLE INFO

Article history:
Received 24 June 2025
Received in revised form
19 Jan. 2026
Accepted 22 Feb 2026
Available online 28 Feb. 2026

Keywords:
Flux-cored arc welding
Heat-affected zone
Microstructure
Post-weld heat treatment
Tensile strength

ABSTRACT

Low-carbon structural steels, such as SS400, are widely used in shipbuilding because of their good weldability, ductility, and adequate strength. However, welding introduces residual stresses and microstructural transformations that may reduce the mechanical performance of welded joints; therefore, post-weld heat treatment (PWHT) is important for improving weld integrity. This study investigated the effect of PWHT temperature on the microstructural evolution and mechanical properties of SS400 steel welded using flux-cored arc welding (FCAW) in the 3G and 4G positions. Welded specimens were subjected to PWHT at 550, 650, and 750°C for 60 min, followed by air cooling, while non-PWHT specimens were used as a reference. Microstructural characterization, hardness testing, and tensile testing were performed to evaluate the mechanical behavior of the welded joints. The base metal and heat-affected zone (HAZ) were predominantly composed of ferrite and pearlite under all conditions, whereas the weld metal exhibited martensite and Widmanstätten ferrite in the lower PWHT range. Among the investigated conditions, PWHT at 550°C produced the most favorable mechanical response, achieving the highest tensile strength of 556 MPa and average hardness values of 191.3 HV in the base metal, 189.3 HV in the HAZ, and 179 HV in the weld metal. The results demonstrate that PWHT temperature significantly influences phase evolution and mechanical performance, with 550°C identified as an effective treatment condition for improving the mechanical reliability of FCAW-welded SS400 joints.

*Corresponding author.
E-mail address: 55824110001@student.mercubuana.ac.id (E. Aprianto)
Peer review under the responsibility of Editorial Board of Jurnal Teknik Mesin Mechanical Xplore (JTMMX)

1. Introduction

Low-carbon structural steel SS400 is extensively utilized in shipbuilding and marine structural applications owing to its favorable weldability, moderate tensile strength, and economic efficiency [1-3]. In ship hull construction, welded joints function as primary load-bearing components that directly influence structural integrity and operational safety. Consequently, the metallurgical stability and mechanical reliability of welded joints are critical factors that determine the service life of marine structures operating under complex loading and corrosive environments. To meet these requirements, welding processes applied in shipyard fabrication must ensure sufficient joint strength and maintain microstructural stability within the weld metal and heat-affected zone (HAZ).

Among the various welding techniques used in marine fabrication, flux-cored arc welding (FCAW) is

https://doi.org/10.36805/nq48my18

one of the most widely adopted processes in shipyard production lines. FCAW offer several advantages, including high deposition rates, deep penetration capability, stable arc characteristics, and good adaptability to automation [4, 5]. In addition, FCAW is particularly suitable for out-of-position welding operations, such as vertical (3G) and overhead (4G) positions, which are frequently encountered during hull assembly and block construction. Despite these advantages, the FCAW process involves intense localized heating followed by rapid cooling, which produces steep thermal gradients across the welded joint. These thermal cycles may induce residual stresses, microstructural heterogeneity, and phase transformations within the weld metal and HAZ [5-7]. Such metallurgical changes can significantly influence the hardness distribution, tensile strength, and fracture behavior, potentially reducing the structural reliability of welded components.

During welding, a rapid thermal cycle can promote the formation of non-equilibrium microstructures, such as martensite, bainite, or Widmanstätten ferrite, particularly in regions experiencing high cooling rates. These phase transformations are often accompanied by significant variations in hardness and local mechanical properties across the welded joint. The heat-affected zone is particularly sensitive to these changes because it undergoes partial austenitization, followed by rapid transformation during cooling. Consequently, controlling the microstructural evolution within the heat-affected zone and weld metal is essential for maintaining mechanical uniformity and preventing premature failure in welded structures.

Post-weld heat treatment (PWHT) is widely employed in welded steel structures to relieve residual stresses and promote microstructural stabilization after welding. PWHT allows diffusion-driven recovery and tempering reactions to occur, which can reduce dislocation density, alleviate internal stresses, and transform unstable phases into more stable ferrite–pearlite structures[6, 8]. Previous studies have reported that PWHT conducted within the temperature range of approximately 550–700°C can effectively reduce the hardness in welded low-carbon steels through tempering reactions, while simultaneously improving ductility and toughness [8-10]. In addition, PWHT may promote the redistribution of carbon and alloying elements, resulting in a more homogeneous microstructure and improved mechanical performance of welded joints.

In addition to the influence of thermal treatment, the welding position also plays an important role in determining the thermal behavior of the molten pool and the cooling characteristics of the weld [3, 11]. Under out-of-position welding conditions, such as 3G and 4G, gravitational effects alter the molten metal flow, arc stability, and heat distribution during welding. These factors can affect the geometry of the weld bead, heat input distribution, and solidification behavior, which ultimately influence the resulting microstructure and mechanical properties of the welded joint. Consequently, welded joints produced in different welding orientations may exhibit variations in hardness distribution, microstructural morphology, and tensile properties, even under similar welding parameters.

Despite extensive research on PWHT effects in welded steel, a significant gap remains regarding the combined influence of welding orientation and PWHT temperature, specifically for FCAW-welded SS400 steel, particularly under out-of-position conditions prevalent in shipyard fabrication. Crucially, the interplay between welding orientation (especially out-of-position conditions common in shipyards) and PWHT temperature on FCAW-welded SS400 has received comparatively limited investigation, leaving a critical knowledge gap in optimizing these processes for structural reliability. Furthermore, the combined influence of welding orientation and PWHT temperature on the microstructural evolution and mechanical properties of FCAW-welded SS400 steel remains unclear. Understanding this interaction is essential because the effectiveness of PWHT in relieving residual stress and stabilizing microstructures may depend on the thermal history generated at different welding positions.

Therefore, in this study, we systematically investigated the effect of PWHT temperature on the microstructure and mechanical performance of SS400 steel welded using the FCAW process in both vertical (3G) and overhead (4G) welding positions. PWHT treatments were conducted at 550, 650, and 750°C to evaluate their influence on the phase transformation behavior, hardness distribution, and tensile strength of the welded joints. The novelty of this research lies in its integrated evaluation of welding position sensitivity and PWHT responsiveness, a critical yet underexplored combination, directly reflecting complex fabrication conditions prevalent in shipyard practice. By establishing the relationship between welding orientation,

PWHT temperature, and resulting mechanical performance, this study provides insights for optimizing post-weld thermal treatment strategies to enhance the structural reliability of marine welded components.

2. Methods

2.1. Materials

The base material used in this study was low-carbon structural steel SS400 with a thickness of 25 mm, classified according to JIS G3101:2015 (rolled steels for general structures). SS400 steel is commonly employed in structural fabrication owing to its favorable weldability, moderate strength, and good ductility, making it suitable for shipbuilding applications.

The chemical compositions and nominal mechanical properties of SS400 are summarized in **Table 1** and **Table 2**, respectively. These properties provide a fundamental reference for evaluating the influence of welding thermal cycles and PWHT on the microstructural evolution and mechanical performance of welded joints.

Table 1. Chemical composition of SS400 structural steel (wt%)

Material	Chemical composition (wt%)				
	C	Si	Mn	P	S
SS400	0.20 – 0.30	≤ 0.50	≤ 1.60	≤0.050	≤0.050

Table 2. Mechanical properties of SS400 steel

Material	Mechanical properties			
	UTS (MPa)	YS (MPa)	EL (%)	Hardness (HV)
SS400	400-510	245	≥21	130 –180

2.2. Welding procedure

Welding was conducted using FCAW) with a metal-active gas (MAG) configuration. The filler metal used in this study was AWS A5.36 E71T1 C1A4 CS1 H8 flux-cored wire, which comprised approximately 14% flux and 86% metallic content. Carbon dioxide (CO_2) was employed as the shielding gas to stabilize the arc and protect the molten pool during welding. The specimens were prepared using a V-butt joint configuration with a groove angle of 60°C and a root gap of 3 mm. Welding was performed in two out-of-position welding orientations, namely, vertical-up (3G) and overhead (4G), to simulate practical welding conditions encountered in ship hull fabrication. A multi-pass welding strategy was applied to ensure adequate joint penetration and bead formation. The welding process consisted of seven layers with a total of 18 passes using a flux-cored wire with a diameter of 1.2 mm. Welding parameters were carefully controlled throughout the process to maintain a consistent heat input and ensure uniform weld quality across all specimens. The schematic configuration of the weld joint and the geometry of the V-butt test specimen used in this study are illustrated in **Figure 1**.

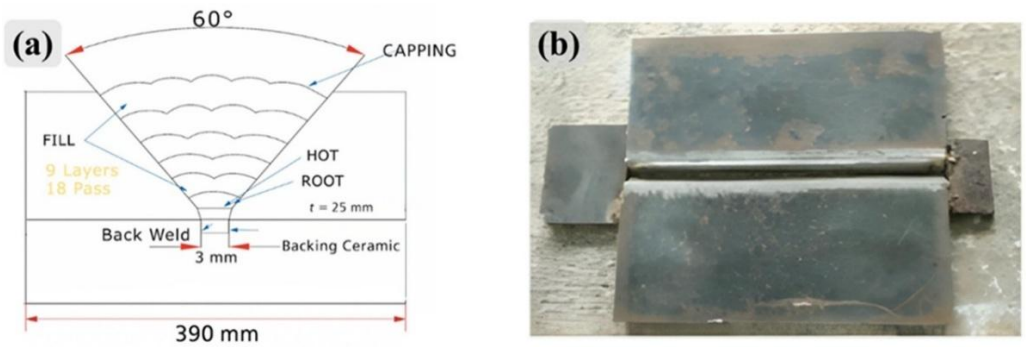

Figure 1. Weld joint configuration: (a) schematic illustration, (b) V-butt joint specimen.

2.3. Welding parameters and heat input

The welding parameters used in this study are summarized in **Table 3**.

Table 3. Welding parameters used in the FCAW process

Parameter	Unit	Value
Welding current	A	180–220
Arc voltage	V	24–28
Travel speed	mm/min	200–300
Wire diameter	mm	1.2
Shielding gas	–	CO_2
Gas flow rate	L/min	15–20

The welding heat input was calculated using Eq. (1), where *HI* is the heat input (kJ/mm), *V* is the arc voltage (V), *I* is the welding current (A), and *S* is the welding travel speed (mm/min).

$$HI = \frac{V \times I \times 60}{1000 \times S} \quad (1)$$

2.4. Post weld heat treatment (PWHT)

After welding, the welded joints were subjected to radiographic inspection in accordance with ASME B31.3 and ASME Section IX standards to detect internal discontinuities, such as porosity, slag inclusions, and incomplete penetration, without damaging the specimens. Only welds that satisfied the acceptance criteria were used for subsequent heat treatment and mechanical testing.

The welded specimens were then classified into four experimental conditions: as-welded (non-PWHT) and PWHT at 550, 650, and 750°C to investigate the effects of PWHT across the subcritical, near-eutectoid, and slightly above-eutectoid temperature ranges relevant to tempering and grain growth in SS400 steel.

Post-weld heat treatment was performed in an electric muffle furnace. The specimens were heated to the target temperature at a controlled heating rate of approximately 10°C/min and maintained at the specified temperature for 60 min. After the holding period, the specimens were removed from the furnace and cooled in air.

2.5. Testing procedures

2.5.1. Metallographic examination

Microstructural characterization was performed using an optical microscope (Nikon MA-100) at a magnification of 500×. The observations focused on the base metal, HAZ, and weld metal regions to evaluate the microstructural evolution following PWHT.

Prior to microscopic examination, the specimens were prepared following standard metallographic procedures, including sectioning, grinding, and polishing. The polished surfaces were etched using a 2% Nital solution in accordance with ASTM E407 to reveal the microstructural constituents, including ferrite, pearlite, and martensitic phases..

2.5.2. Hardness testing

Figure 2 shows the hardness measurements were performed using a Vickers hardness tester (MHRV-50AT, s/n: 17043). The tests were conducted in accordance with ASTM E92:2017 using a load of 10 kgf. Indentations were performed along the transverse cross-section of the welded joint, covering the weld metal, HAZ, and base metal. Measurements were taken at regular intervals to obtain the hardness distribution across the welded joint. For each region, three measurements were recorded and averaged to determine the

representative hardness value.

Figure 2. A Mitech HVS-50AT micro-Vickers hardness tester was used for the hardness measurements.

2.5.3. Tensile testing

Tensile tests were conducted using an Instron universal testing machine (electromechanical dual-column system) in accordance with the ASTM A370 standard. Standard tensile specimens were machined from the welded plates with the weld located at the center of the gauge section.

Tests were performed to determine the ultimate tensile strength (UTS), yield strength (YS), and percentage elongation of the welded joints. The specimen geometry used in the tensile test is illustrated in Figure 3. All experimental results were systematically analyzed to establish correlations between the PWHT temperature, microstructural evolution, and mechanical behavior of the FCAW-welded SS400 steel.

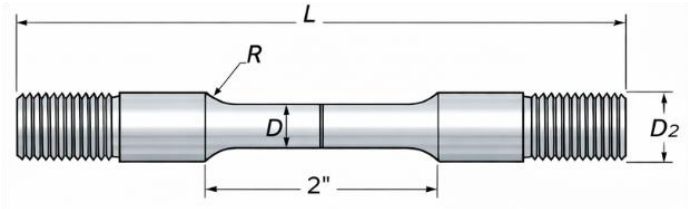

Figure 3. The geometry of the tensile test specimens was determined according to ASTM A370.

3. Result and Discussions

3.1. Welding results

The FCAW welding process successfully produced welded joints in SS400 steel plates using a V-butt joint configuration with a 60° groove angle and a 3 mm root gap. Welding was performed in two out-of-position orientations, namely, vertical-up (3G) and overhead (4G), using a multi-pass technique consisting of seven layers and eighteen passes. The resulting weld beads generally exhibited continuous fusion and acceptable bead geometry, indicating stable welding conditions throughout the process.

Radiographic inspection revealed noticeable differences in the weld quality between the two welding positions. Welded joints produced in the vertical-up (3G) position exhibited relatively small porosity and adequate penetration, remaining within the acceptance limits specified by AWS D1.1 and ASME Section IX standards [12], as further detailed and visualized in Figure 5a. The weld beads in this position also showed a relatively uniform geometry with minimal surface irregularities, suggesting stable molten-pool behavior and effective control of the welding parameters.

In contrast, specimens welded in the overhead (4G) position exhibited a higher tendency to have welding defects, including larger porosity and localized incomplete penetration. Some of these imperfections

exceeded the acceptable limits defined by the welding standards. The increased defect formation at the 4G position can be attributed to the influence of gravity on the molten weld pool, which reduces weld pool stability and makes it more difficult to maintain consistent penetration and slag removal during welding. Consequently, controlling the molten metal flow and solidification becomes more challenging in overhead welding than in vertical-up welding.

These observations are consistent with previous studies reported in the literature. For example, [4] reported that FCAW applied to structural steel plates in the 3G position tends to produce stable bead geometry and high weld integrity when appropriate welding parameters are used. Similarly, [13] observed that variations in welding current and travel speed significantly affect bead formation and defect generation in FCAW welded carbon steels. Therefore, the results presented herein confirm that welding orientation plays a significant role in determining weld quality and defect formation.

After radiographic inspection, welded specimens that met the acceptance criteria were selected for further characterization. These specimens were subsequently subjected to metallographic examination, hardness testing, and tensile testing to investigate the influence of PWHT temperature on the microstructural evolution and mechanical performance of the FCAW-welded SS400 joints, as illustrated in Figure 4.

Figure 4. Welding result

3.2. Radiographic test result analysis

Radiographic inspection was performed to evaluate the internal weld quality and identify discontinuities in the welded joints. The results indicate that welding orientation significantly affects defect formation and weld integrity. In the vertical-up (3G) welding position, only minor porosity indications were observed, and these remained within the acceptance limits specified by AWS D1.1 and ASME Section IX standards [12, 14]. The upward progression of the weld pool during vertical welding contributes to a relatively stable arc behavior and controlled penetration, which promotes more uniform solidification of the weld metal. The corresponding radiographic film at the 3G welding position is shown in Figure 5a.

The occurrence of low porosity in FCAW welds is commonly associated with gas entrapment during weld metal solidification. Previous studies on SS400 welding have reported that porosity and small voids may develop when the welding parameters, particularly the welding current and arc stability, are not fully optimized. Such defects are generally caused by fluctuations in the shielding gas protection or disturbances in the molten weld pool during solidification. Radiographic examinations typically reveal these defects as dark circular indications on the film, representing localized gas cavities trapped in the weld metal [9, 15]. Although a small porosity may still fall within acceptable limits according to welding standards, its presence indicates localized instability in the welding process.

In contrast, welds produced in the overhead (4G) position exhibited a higher tendency for internal defects, including more pronounced porosity and localized incomplete penetration, as illustrated in Figure

5b. The increased defect susceptibility in overhead welding is primarily attributed to the influence of gravity acting against the support of the molten weld pool. This condition reduces weld pool stability and makes it more difficult to maintain consistent metal transfer and slag removal during welding. Consequently, gas entrapment and irregular bead formation are more likely to occur.

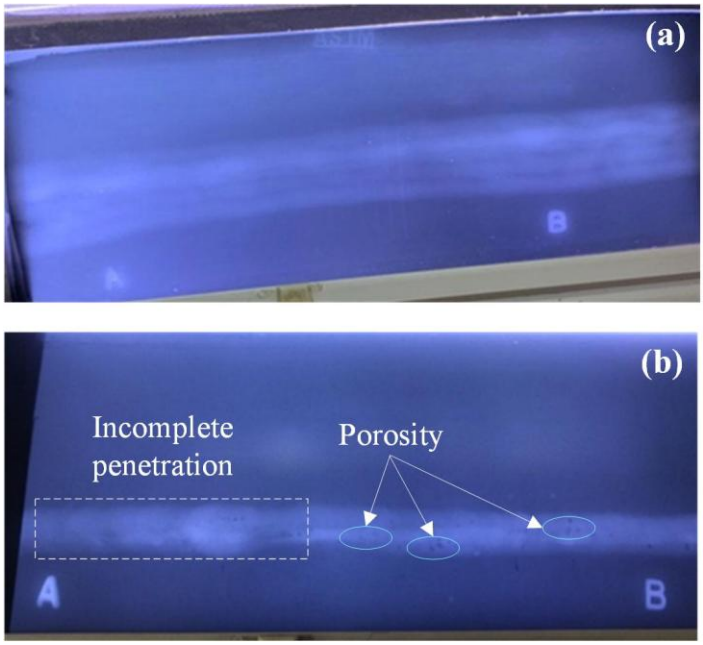

Figure 5. Radiographic test results of welded joints showing internal defects: (a) 3G welding position and (b) 4G welding position.

These observations are consistent with those of previous studies. Out-of-position welding has been demonstrated to significantly alter the heat flow direction, molten metal dynamics, and cooling behavior during solidification. Such changes may also influence defect formation and the resulting microstructural characteristics of the welded joint [4, 16, 17]. Because the cooling rate and thermal gradients directly affect the phase transformation pathways in low-carbon steels, welding orientation becomes an important factor when combined with PWHT. Therefore, understanding the interaction between welding position and thermal treatment is essential for improving weld quality and ensuring the structural reliability of welded components in shipbuilding applications. Although this study provides valuable insights, it has certain limitations. The PWHT holding time was fixed at 60 min, and the cooling method was air cooling. Although these provided a baseline, variations in holding time could impact the extent of diffusion-driven processes, and different cooling rates might influence the final phase composition, potentially altering the observed microstructural evolution and mechanical response. Furthermore, the study focused on static mechanical properties (hardness and tensile strength). For marine applications, dynamic properties such as fatigue or impact toughness are crucial for structural integrity under operational loads, and long-term corrosion resistance is vital in harsh environments. Future work should investigate these aspects to provide a more comprehensive assessment of service life.

3.3. Metallographic observation analysis

Microstructural observations were conducted using an optical microscope at 500× magnification to evaluate the structural evolution of SS400 steel before and after PWHT at temperatures of 550, 650, and 750°C, followed by air cooling. The base metal of SS400 steel exhibited a typical ferrite–pearlite microstructure, characteristic of low-carbon structural steels [1-3]. Ferrite appeared as the dominant soft phase, while pearlite was distributed as lamellar colonies within the ferritic matrix. This microstructural configuration corresponds to the moderate hardness range (approximately 130–180 HV) commonly reported for SS400 steel.

Figure 6 shows microstructural observations of SS400 steel under non-PWHT (Figure 6a) and PWHT conditions at temperatures of 550, 650, and 750°C (Figure 6b, c, and d, respectively**Figure 6Figure 6Figure 6**). After PWHT at 550°C, the microstructure showed slight grain refinement and improved phase uniformity. Because this temperature is below the eutectoid transformation temperature ($A_1 \approx 727$°C), austenitization did not occur. Instead, recovery processes dominated, resulting in a reduction in internal stress and dislocation density while maintaining the stability of the ferrite– pearlite structure [6].

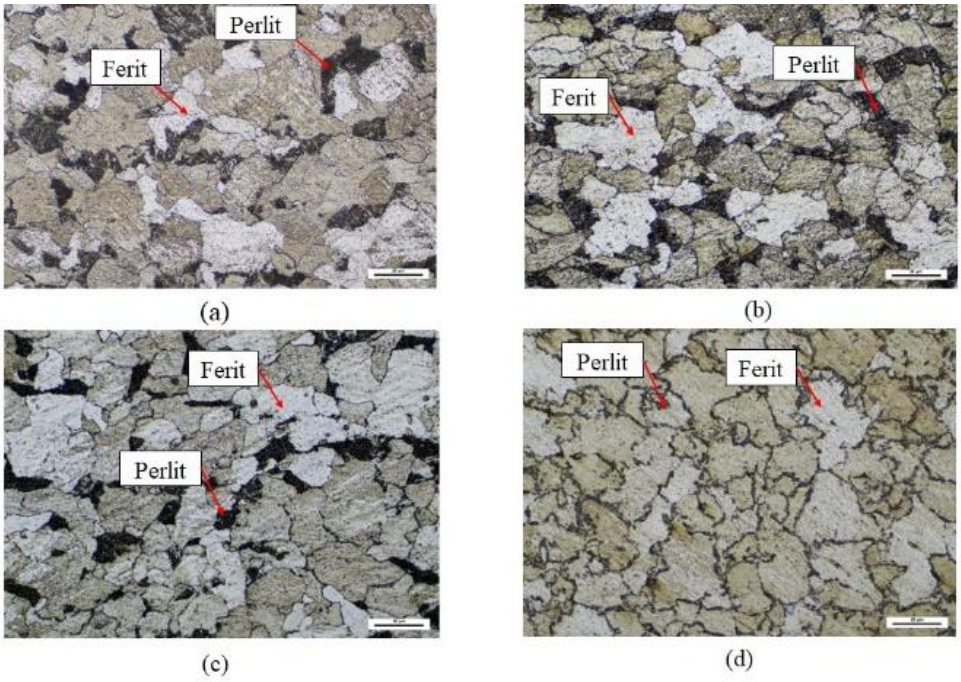

Figure 6. Microstructures of the base metal under different PWHT conditions: (a) non-PWHT, (b) 550°C, (c) 650°C, (d) 750°C.

When the PWHT temperature increased to 650°C and 750°C, grain boundary mobility increased due to enhanced atomic diffusion. This promoted ferrite grain coarsening, particularly at 750°C where diffusion-driven grain growth became more pronounced, as visibly indicated by the larger, less defined grains in Figure 6d compared to Figure 6b. Similar grain coarsening behavior at elevated PWHT temperatures has been reported for SS400 and other mild steels [1, 6]. The grain growth process can be explained by thermally activated grain boundary migration, in which larger grains progressively consume smaller grains to reduce the total grain boundary energy of the system. Consequently, the coarsened microstructure reduces resistance to dislocation movement, which subsequently affects the hardness and tensile properties of the welded material.

As shown in Figure 7, the microstructure of the heat-affected zone (HAZ) changed significantly with increasing PWHT temperature. The HAZ experienced intense thermal cycling during welding, resulting in heterogeneous microstructural characteristics. In the as-welded condition, rapid cooling produced a nonuniform ferrite–pearlite distribution with localized hardened regions caused by partial phase transformations.

PWHT at 550°C promoted tempering reactions within the HAZ, facilitating the redistribution of carbon atoms and stabilizing the ferrite–pearlite structure (Figure 7b). This process reduces internal residual stresses while maintaining microstructural stability. Similar stabilization effects have been reported in previous studies on mild steel welds [6, 8].

As the PWHT temperature increased, diffusion-controlled processes became more dominant. At 750°C, the ferrite grains in the HAZ exhibited significant coarsening accompanied by partial cementite spheroidization (Figure 7d). This temperature approaches the eutectoid transformation region, thereby increasing the atomic mobility and promoting microstructural homogenization. Comparable diffusion-driven microstructural evolution in mild steel welds subjected to elevated PWHT has been reported [4, 10].

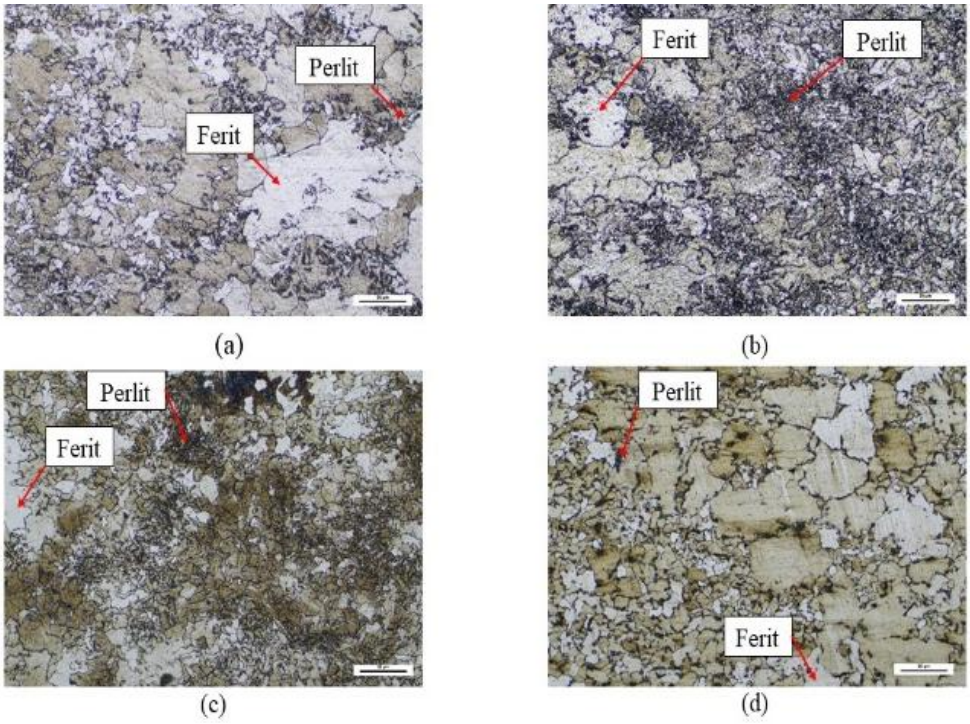

Figure 7. Microstructures of the heat-affected zone (HAZ) under different PWHT conditions: (a) non-PWHT, (b) 550°C, (c) 650°C, and (d) 750°C.

Overall, the HAZ microstructure demonstrated a clear temperature-dependent transition, evolving from stress relief and microstructural stabilization at 550°C to diffusion-dominated grain coarsening at higher temperatures. This evolution indicates that the PWHT temperature plays a critical role in controlling the microstructural stability and the subsequent mechanical behavior of welded SS400 steel [12].

The weld metal in the non-PWHT condition (Figure 8a) exhibited martensitic features and a Widmanstätten ferrite morphology. These structures were formed as a result of rapid cooling from the molten state during solidification, which generated a high dislocation density and significant residual stress concentration. Similar microstructural features have been reported in low-carbon steel weldments subjected to rapid solidification [4, 6].

After PWHT at temperatures of 550–650°C, tempering reactions occurred within the weld metal, reducing the martensitic tetragonality and promoting partial transformation into ferrite and stabilized pearlite (Figure 8b–c). This tempering process facilitates carbon redistribution and reduces internal stresses, resulting in improved phase uniformity without significant grain coarsening. Comparable tempering behavior has been reported in previous studies on SS400 welded joints [1].

At the higher PWHT temperature of 750°C, diffusion-controlled processes became dominant. Extensive atomic diffusion promoted cementite spheroidization and gradual transformation of the microstructure into coarser ferritic grains (Figure 8d). The breakdown of the lamellar pearlite structure into spheroidized cementite reduced the strength of the weld metal but improved its ductility. This metallurgical evolution is consistent with the findings of [10, 18], who reported mechanical softening in low-carbon steel weld metals subjected to elevated PWHT.

3.4. Hardness test result analysis

The hardness test was conducted using the Vickers method in accordance with ASTM E92:2017, utilizing a Mitech Micro Vickers Hardness Tester model HVS-1000A. The instrument provides a measurement resolution of 0.1 HV, an indenter load accuracy within ±1%, and a reading precision of approximately ±0.5 HV, ensuring reliable hardness measurements [19]. Hardness measurements were performed across the base metal (BM), HAZ, and weld metal (WM) under non-PWHT conditions and after PWHT at 550, 650, and 750°C. The results are summarized in Table 4.

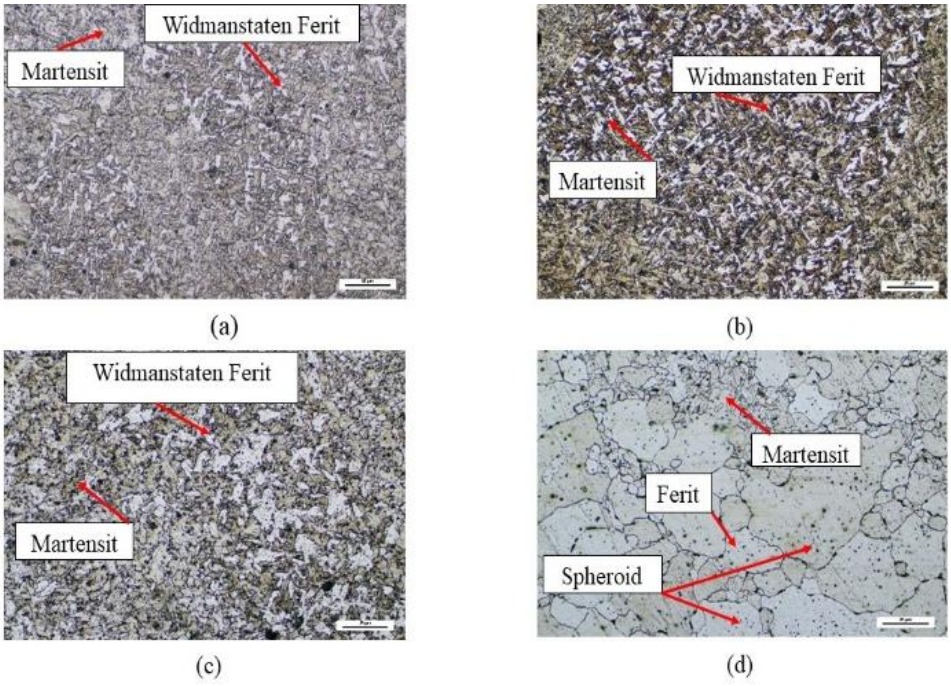

Figure 8. Microstructures of the weld metal under different PWHT conditions: (a) non-PWHT, (b) 550°C, (c) 650°C, (d) 750°C.

As shown in Table 4, the hardness values in all regions gradually decreased with increasing PWHT temperature. In the non-PWHT condition, the average hardness values were 194 HV in the base metal, 192.6 HV in the HAZ, and 185.6 HV in the weld metal. After PWHT at 550°C, the hardness slightly decreased to 191.3 HV in the BM, 189.3 HV in the HAZ, and 179 HV in the WM. A further decrease was observed at 650°C and 750°C, where the average hardness values reached 188.3 HV and 174.3 HV in the base metal, 186 HV and 174 HV in the HAZ, and 178 HV and 168 HV in the weld metal, respectively. This gradual reduction indicates that increasing PWHT temperature promotes microstructural softening in the welded joint.

Table 4. Hardness test result data

Material	Test Location	Point	Vickers Hardness Number (HV) Test Load Applied 10 Kgf			
			Non PWHT	PWHT 550°C	PWHT 650°C	PWHT 750°C
SS400	Base Metal (BM)	1	201	169	166	145
		2	201	202	199	186
		3	221	203	200	192
		Average	194	191.3	188.3	174.3
	HAZ	1	170	163	159	149
		2	188	200	197	186
		3	220	205	202	187
		Average	192.6	189.3	186	174
	Weld Metal	1	158	161	160	145
		2	186	178	184	180
		3	213	198	190	179
		Average	185.6	179	178	168

The relatively higher hardness in the non-PWHT condition was associated with the presence of martensitic structures and residual stresses generated during rapid cooling after welding. Rapid solidification produces a high dislocation density and lattice distortion, which increases the resistance to plastic deformation and indentation. Similar hardness characteristics in as-welded low-carbon steel joints have been reported by [1, 6, 7].

Moderate hardness reduction occurred with recovery and tempering reactions that reduced lattice distortion and dislocation density within the microstructure upon PWHT at 550°C. These processes facilitated carbon redistribution and stabilized the ferrite–pearlite phases without significant grain

coarsening. Comparable hardness reductions in SS400 weldments subjected to subcritical PWHT have been reported elsewhere [8].

At higher PWHT temperatures, particularly 750°C, the hardness decreased more noticeably. Elevated temperatures accelerate atomic diffusion, promoting ferrite grain growth and cementite spheroidization. This microstructural coarsening weakens the grain-boundary strengthening mechanisms. According to the Hall–Petch relationship, an increase in grain size reduces the resistance to dislocation motion, thereby lowering the hardness and yield strength of the material [4]. Similar diffusion-driven softening in mild steel weldments subjected to elevated PWHT temperatures has been previously reported [20, 21].

Overall, the hardness behavior observed in this study confirms that PWHT primarily acts as a stress-relief and softening treatment for FCAW-welded SS400 steel. Among the investigated conditions, PWHT at 550°C provides a balanced effect by reducing residual stresses while maintaining relatively stable microstructural characteristics.

3.5. Tensile test result analysis

The microstructure formed during the welding process and the subsequent post-weld heat treatment (PWHT) significantly influence the mechanical properties of SS400 steel, particularly its tensile strength. Tensile testing was conducted at PT Detech Professional Indonesia, and the results showed that all welded specimens, both without PWHT and with PWHT at temperatures of 550, 650, and 750°C, exhibited higher tensile strengths than the raw material [6, 22-25]. The tensile strength values for each condition are shown in Figure 9.

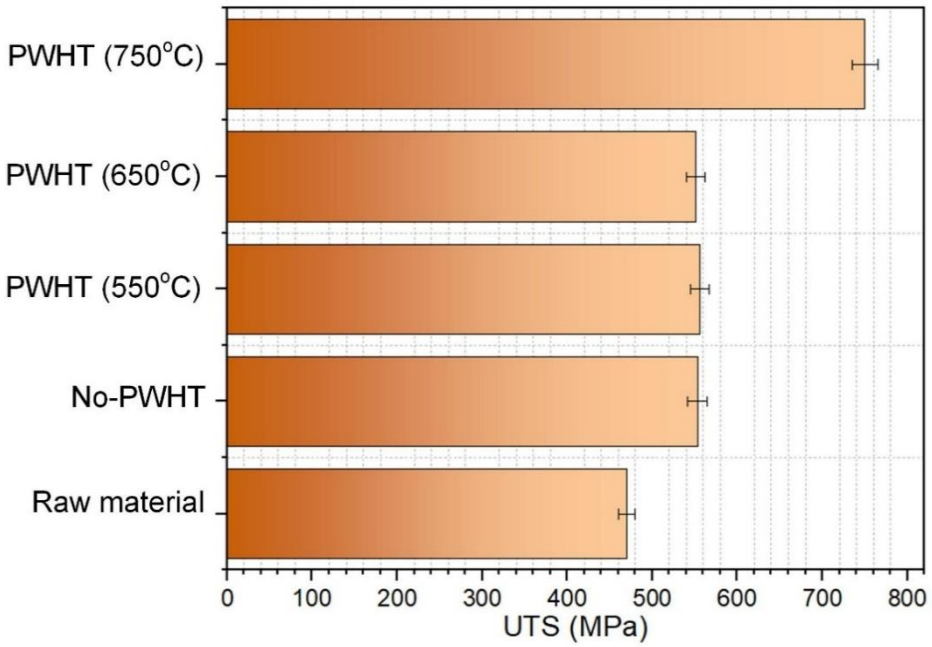

Figure 9. Tensile test results under different PWHT and non-PWHT conditions.

The experimental results indicate that the PWHT temperature has a notable effect on the ultimate tensile strength (UTS) of the welded joints. The highest tensile strength was obtained at a PWHT temperature of 550°C, reaching 556 MPa. This value slightly exceeds the tensile strength under the non-PWHT condition (553 MPa). However, when the PWHT temperature increased to 650 and 750°C, the tensile strength decreased to 551 and 505 MPa, respectively.

The improvement in the tensile strength at 550°C can be attributed to effective residual stress relaxation combined with microstructural stabilization in the weld metal and heat-affected zone. At this subcritical temperature, tempering reactions reduce the lattice distortion and dislocation density while maintaining relatively fine ferrite–pearlite structures. This controlled stress redistribution enhances the load

transfer across the welded joint without inducing excessive grain coarsening. Similar improvements in tensile performance under moderate PWHT conditions have been reported in previous studies on low-carbon steel weldments [1, 6].

As the PWHT temperature increased to 650 and 750°C, the tensile strength gradually decreased. This reduction corresponds to the microstructural evolution observed in the metallographic analysis, particularly ferrite grain coarsening and cementite spheroidization. Elevated thermal exposure increases atomic diffusion, which reduces the dislocation density and weakens the grain boundary strengthening mechanisms. Consequently, the welded joint experienced mechanical softening and a reduction in tensile strength. Comparable strength degradation due to excessive PWHT temperatures has been reported in mild steel welds [10, 15-18].

The tensile behavior observed in this study is consistent with the hardness trends discussed in the previous section, wherein an increase in the PWHT temperature resulted in the gradual softening of the material. Among the investigated conditions, PWHT at 550°C affords the most favorable mechanical response for FCAW-welded SS400 steel. At this temperature, residual stresses are effectively relieved, whereas the microstructure remains relatively stable, thereby maintaining a balanced combination of strength and ductility. In contrast, higher PWHT temperatures promote diffusion-driven grain growth and metallurgical homogenization, which ultimately reduces the tensile performance of the welded joint.

Overall, the combined microstructural, hardness, and tensile test results demonstrate a clear relationship between the PWHT temperature and the mechanical performance of FCAW-welded SS400 steel. Metallographic observations revealed that moderate PWHT at 550°C promoted microstructural stabilization through recovery and tempering processes without significant grain coarsening. This condition maintained a relatively refined ferrite–pearlite structure in the base metal and HAZ, while tempering the martensitic features in the weld metal. Consequently, the welded joint exhibited balanced mechanical behavior, characterized by moderate hardness reduction and the highest tensile strength. In contrast, higher PWHT temperatures (650–750°C) accelerated diffusion-controlled processes, such as ferrite grain growth and cementite spheroidization, which weakened grain boundary strengthening mechanisms and led to gradual softening. These findings indicate that the mechanical response of the welded joint is strongly governed by the evolution of the microstructure during PWHT. Therefore, a PWHT temperature of approximately 550°C provides the most favorable balance between residual stress relief, microstructural stability, and tensile performance for FCAW-welded SS400 steel.

4. Conclusion

This study investigated the influence of post-weld heat treatment (PWHT) temperature on the microstructure and mechanical properties of SS400 structural steel welded using flux-cored arc welding (FCAW). A key finding and practical limitation was that the welding position significantly affected weld quality; while the 3G position consistently produced welds meeting the acceptance criteria, the 4G position demonstrated higher susceptibility to porosity and incomplete penetration, indicating challenges for consistent quality control in this orientation. PWHT temperature strongly influenced the microstructural evolution and mechanical behavior of the welded joints. Among the investigated conditions, PWHT at 550°C produced the highest tensile strength (556 MPa) and a relatively stable hardness distribution across the base metal, heat-affected zone, and weld metal owing to effective residual stress relaxation and microstructural stabilization through tempering. In contrast, higher PWHT temperatures (650–750°C) promoted ferrite grain coarsening and cementite spheroidization, resulting in reduced hardness and tensile strength because of diffusion-driven microstructural softening. Therefore, PWHT at 550°C for 60 min, followed by normalizing cooling, provides the most favorable balance between microstructural stability and mechanical performance, making it a suitable heat treatment condition for FCAW-welded SS400 steel used in structural applications such as shipbuilding.

Author's Declaration

Authors' contributions and responsibilities

Edo Aprianto was responsible for the conceptualization, methodology, experimental work, data analysis, and writing the original draft. **Haftirman** supervised the research and provided technical guidance and validation.

Acknowledgment

The authors would like to express their sincere gratitude to all parties who provided support, guidance, and assistance throughout the preparation and completion of this manuscript. Their valuable contributions, both direct and indirect, are greatly appreciated.

Availability of data and materials

All data supporting the findings of this study are available from the corresponding author upon reasonable request.

Competing interests

The authors declare no conflicts of interest related to this study.

References

[1] N. MUHAYAT, S. YASINTA, A. R. PRABOWO, Y. C. N. SAPUTRO, and T. TRIYONO, "EFFECT OF THE POST WELD HEAT TREATMENT ON THE MICROSTRUCTURE OF THE UNDERWATER WET WELDING SS400 STEEL," *HRČAK,* vol. 62, pp. 20-22, 2025.

[2] J. Sutanto, I. Iswanto, I. Sumirat, A. Pramutadi Andi Mustari, and S. Permana, "Development of Standard Test Specimens for Competency Improvement of Non-destructive Test (NDT) Personnel—Industrial Radiography," *JMPM (Jurnal Material dan Proses Manufaktur),* vol. 9, no. 2, pp. 116-124, 2025. doi: https://doi.org/10.18196/jmpm.v9i2.26290

[3] F. W. Pribadi and N. S. Drastiawati, "PENGARUH VARIASI TEMPERATUR DALAM PROSES PWHT PENGELASAN SMAW UNTUK MATERIAL BAJA SS400 TERHADAP NILAI KEKUATAN TARIK DAN KEKUATAN IMPAK," *Jurnal Teknik Mesin,* vol. 12 no. 2, pp. 17-22, 2024.

[4] B. Bagheri Vanani, M. R. Mehraban Dehaqani, M. Abbasi, M. Sadeqi Bajestani, M. Mohammadkhah, and S. Klinge, "Effects of PWHT on the microstructure, corrosion, tribology, and mechanical properties of mild steel welds under different joining positions: Experimental and Numerical Study," *Journal of Materials Research and Technology,* vol. 38, pp. 752-767, 2025. doi: https://doi.org/10.1016/j.jmrt.2025.07.253

[5] B. X. Guo, X. W. Du, and J. Hu, "Study on TIG and SMAW Comprehensive Welding Process of 1Cr18Ni9Ti/Q235 Compound Steel," *Advanced Materials Research,* vol. 487, pp. 371-374, 2012. doi: https://doi.org/10.4028/www.scientific.net/AMR.487.371

[6] I. O. Oladele, D. B. Alonge, T. O. Betiku, E. O. Igbafen, and B. O. Adewuyi, "Performance Evaluation of the Effects of Post Weld Heat Treatment on the Microstructure, Mechanical and Corrosion Potentials of Low Carbon Steel," *Advanced Technologies & Materials,* vol. 44, no. 1, pp. 41-47, 2019. doi: https://doi.org/10.24867/atm-2019-1-007

[7] Khoirudin, K. Karyadi, A. Kusnadi, A. Amir, A. Abdulah, A. Hananto, and M. Taufik Ulhakim, "Taguchi-Based Optimization of TIG Welding for Joining Low-Carbon Steel (ST37) and Stainless Steel (SUS 304)," *Jurnal Teknik Mesin Mechanical Xplore,* vol. 5, no. 2, pp. 88-101, 2025. doi: https://doi.org/10.36805/jtmmx.v5i2.9043

[8] M. F. I. Purba, A. Fathier, and F. Fakhriza, "Pengaruh variasi temperatur PWHT dan tanpa PWHT terhadap sifat kekerasan baja ASTM A106 grade B pada proses pengelasan SMAW," *Journal of*

Welding Technology, vol. 2, no. 1, 2020. doi: http://dx.doi.org/10.30811/jowt.v2i1.1132

[9] D. Kim and B.-H. Shin, "Study on Electrochemical Behavior at a Room and High Temperature at 700 °C Corrosion of Austenite, Ferrite, and Duplex Stainless Steels," *Metals,* vol. 16, no. 1, 2026. doi: https://doi.org/10.3390/met16010082

[10] J. Xiong, T. Li, X. Yuan, G. Mao, J. Yang, L. Yang, and J. Xu, "Improvement in Weldment of Dissimilar 9% CR Heat-Resistant Steels by Post-Weld Heat Treatment," *Metals,* vol. 10, no. 10, 2020. doi: https://doi.org/10.3390/met10101321

[11] E. Aprianto and H. Pranoto, "Literature Review on Microstructure and Mechanical Properties of Ss400 Steel Due To Variations in PWHT Temperature in the GMAW Welding Process," *nternational Journal of Advanced Technology in Mechanical, Mechatronics and Materials,* vol. 06, no. 2, pp. 107-118, 2025. doi: https://doi.org/10.37869/ijatec.v6i2.129

[12] *AWS D1.1/D1.1M:2025 An American National Standard*, 2025.

[13] B. Singh, S. S. Sandhu, and A. Doomra, "Effect of post weld heat treatment on metallurgical and mechanical properties of electron beam welded AISI 409 ferritic steel," *Metallurgical and Materials Engineering,* vol. 26, no. 3, pp. 279-292, 2020. doi: https://doi.org/10.30544/545

[14] *BPVC Section IX Welding Brazing and Fusing Qualifications*, 2015.

[15] R. Wang, L. Zhu, H. Liu, J. Du, H. Liu, and L. Hu, "Effect of Post-weld Heat Treatment on Microstructure and Mechanical Properties of P91 Heat-Resistant Steel Coating on Mild Steel," *Journal of Materials Engineering and Performance,* vol. 34, no. 5, pp. 4105-4115, 2024. doi: https://doi.org/10.1007/s11665-024-09420-8

[16] A. Moorthy, D. Subbiah, M. Nallusamy, S. Myilsamy, M. Durairaj, and K. Ramaswamy, "Comprehensive investigation on the influence of friction welding parameters on the mechanical integrity, microstructural evolution, and phase stability of AISI 304 austenitic stainless-steel joints," *The International Journal of Advanced Manufacturing Technology,* vol. 142, no. 11-12, pp. 6005-6015, 2026. doi: https://doi.org/10.1007/s00170-026-17465-3

[17] R. Rusiyanto, W. Widayat, and D. D. Saputro, "PENGARUH VARIASI SUHU POST WELD HEAT TREATMENT ANNEALING TERHADAP SIFAT MEKANIS MATERIAL BAJA EMS-45 DENGAN METODE PENGELASAN SHIELDED METAL ARC WELDING (SMAW)," *Jurnal Sain dan Teknologi,* vol. 10, no. 1, pp. 83-89, 2012.

[18] Y. B. Li, "Effect of PWHT process on carbide precipitation behavior and impact toughness of pressure vessel steel," *Sci Rep,* vol. 15, no. 1, p. 9735, Mar 21 2025. doi: https://doi.org/10.1038/s41598-025-94900-7

[19] Siswanto, Sukarman, D. Mulyadi, Khoirudin, R. A. Nanda, A. Abdulah, A. D. Shieddieque, and S. D. Prasetyo, "Box-Behnken Response Surface Methodology: An Analysis of the Effect of Variations in TIG Welding Parameters on Tensile Strength and Hardness Using SUS 304 Material," *Annales de Chimie - Science des Matériaux,* vol. 48, no. 3, 2024. doi: https://doi.org/10.18280/acsm.480302

[20] H. P. Pydi, A. Pradeep, S. Vijayakumar, and R. Srinivasan, "Examination of various weld process parameters in MIG welding of carbon steel on weld quality using radiography & magnetic particle testing," *Materials Today: Proceedings,* vol. 62, pp. 1909-1912, 2022. doi: https://doi.org/10.1016/j.matpr.2022.01.160

[21] A. K. Sk, R. B. P, R. K. B, and S. K. A, "Evaluation of friction welded dissimilar pipe joints between AISI 4140 and ASTM A 106 Grade B steels used in deep exploration drilling," *Journal of Manufacturing Processes,* vol. 56, pp. 197-205, 2020. doi: https://doi.org/10.1016/j.jmapro.2020.04.078

[22] N. R. Oktaviandy, K. Kardiman, and R. Hanifi, "Effect of Preheat Temperature Variation with Cooling Media on Mechanical Properties in Welding SS400 Steel," *SINTEK JURNAL: Jurnal Ilmiah Teknik Mesin,* vol. 17, no. 2, 2023. doi: https://doi.org/10.24853/sintek.17.2.130-142

[23] L. Song, Y. Peng, H. Zhao, and Y. Cao, "The Influence Mechanism of HSLA Weld Metal with Different Composition on High-Temperature Strength," *Advanced Engineering Materials,* vol. 24,

no. 8, p. 2101549, 2022/08/01 2022. doi: https://doi.org/10.1002/adem.202101549

[24] W. Yu, M. Fan, J. Shi, F. Xue, X. Chen, and H. Liu, "A comparison between fracture toughness at different locations of SMAW and GTAW welded joints of primary coolant piping," *Engineering Fracture Mechanics,* vol. 202, pp. 135-146, 2018. doi: https://doi.org/10.1016/j.engfracmech.2018.09.021

[25] A. Sumesh, L. V. S. Ramnadh, P. Manish, V. Harnath, and V. Lakshman, "A Computational approach in optimizing process parameters of GTAW for SA 106 Grade B steel pipes using Response surface methodology," *IOP Conference Series: Materials Science and Engineering,* vol. 149, 2016. doi: https://doi.org/10.1088/1757-899x/149/1/012038